JACS
JOURNAL OF THE AMERICAN CHEMICAL SOCIETY

COMMUNICATION

pubs.acs.org/JACS

CO-Induced Embedding of Pt Adatoms in a Partially Reduced FeO_x Film on Pt(111)

Lindsay R. Merte,[†] Jan Knudsen,[†,#] Falk M. Eichhorn,[‡] Soeren Porsgaard,[†] Helene Zeuthen,[†] Lars C. Grabow,[‡,▽] Erik Lægsgaard,[†] Hendrik Bluhm,[§] Miquel Salmeron,[∥,⊥] Manos Mavrikakis,[‡] and Flemming Besenbacher*[,†]

[†]Interdisciplinary Nanoscience Center (iNANO) and Department of Physics and Astronomy, Aarhus University, DK-8000 Aarhus C, Denmark

[‡]Department of Chemical and Biological Engineering, University of Wisconsin-Madison, Madison, Wisconsin 53706, United States

[§]Chemical Sciences Division and [∥]Materials Science Division, Lawrence Berkeley National Laboratory, Berkeley, California 94720, United States

[⊥]Department of Materials Science and Engineering, University of California, Berkeley, California 94720, United States

Supporting Information

ABSTRACT: The reduction of a single-layer FeO film grown on Pt(111) by CO at elevated pressures and temperatures has been studied through an interplay of scanning tunneling microscopy, ambient-pressure X-ray photoelectron spectroscopy, and density functional theory calculations. Exposure of the FeO thin film to CO at pressures between 1 and 30 Torr and temperatures between 500 and 530 K leads to formation of a honeycomb-structured Fe_3O_2 film with hollow sites occupied by single Pt atoms extracted from the substrate surface. The formation of these adatoms is driven by an increase in CO adsorption energy. In addition, the structure incorporates undercoordinated Fe centers, which are proposed to have substantial effects on the catalytic properties of the surface.

Knowledge of the surface structure of catalytic materials under realistic temperature and pressure conditions is crucial for obtaining an atomistic understanding of the reaction mechanisms of heterogeneous catalysts. Exposure to reactant molecules, especially at elevated pressures and temperatures, may cause substantial surface restructuring, leading to the breaking of metal−metal bonds.[1−7] As a result, the catalytic properties of the material are changed. Thus, studies of surfaces under ultrahigh vacuum (UHV) conditions may fail to reproduce in a realistic way the processes occurring on real catalysts.

Contributing further to the complexity of such systems is the addition of promoter materials to the catalyst, either in the form of so-called "active supports" or as additives to the supported catalyst. The presence of iron in platinum-based catalysts has been shown to enhance their catalytic activity for several reactions, including the preferential oxidation of CO in hydrogen (PROX),[8−11] the oxygen reduction reaction (ORR),[12−14] and the water-gas shift (WGS) reaction.[15,16] The promotional effects of Fe have been attributed in some cases to alloy formation, which modifies the electronic structure of the Pt and thus its chemisorption behavior,[9−11,13] and in others to metal−oxide interface effects such as charge transfer or the creation of complementary reactive sites on the metal and oxide surfaces.[8,17]

Clearly, the relative importance of such effects depends not only on the structure of the catalyst synthesized but also on the reaction conditions, as Fe can exist in a number of different chemical states. Thus, to understand the catalytic behavior of such promoted catalysts, it is mandatory to determine the detailed atomic-scale surface structure of different Fe/Pt systems in situ under reaction conditions.

Recently, Sun, Giordano, and co-workers showed that under strongly oxidizing conditions and total pressures in the millibar range, a monolayer FeO film on Pt(111) is transformed into a trilayer FeO_2 phase, which is reported to be highly active for CO oxidation.[18−20] However, in some reactions, including PROX, for which Fe/Pt has been shown to be a very active catalyst,[11,21] strongly reducing conditions are employed, and the catalytic activity and selectivity are largely determined by the energetics of adsorption of CO on the surface.[22] We therefore undertook the present study in order to determine the structural changes that occur in similar FeO films at high CO pressures, where oxygen-deficient phases rather than oxygen-rich ones may form. In particular, we compared the FeO_x phases found at high CO pressures with the surprisingly stable substoichiometric FeO_x films observed in previous studies after reduction with atomic hydrogen under UHV conditions.[23,24]

Scanning tunneling microscopy (STM) measurements were carried out using the Aarhus scanning tunneling microscope[25] mounted in a UHV chamber with a directly attached, gold-plated high-pressure cell wherein CO exposures were performed. The in situ ambient-pressure X-ray photoelectron spectroscopy (AP-XPS) measurements[26,27] were performed at beamline 11.0.2 at the Advanced Light Source[28] at Lawrence Berkeley National Laboratory, where XPS spectra were recorded at total pressures up to ∼1 Torr. In both the STM and AP-XPS experiments, the FeO thin films were prepared by deposition and oxidation of Fe onto an atomically clean and flat Pt(111) single-crystal surface.[29−31] Density functional theory (DFT) calculations were carried out in slab supercell geometry using the VASP code,[32,33] employing the PW91 exchange−correlation functional,[34] the on-site Hubbard U

Received: February 20, 2011
Published: June 27, 2011

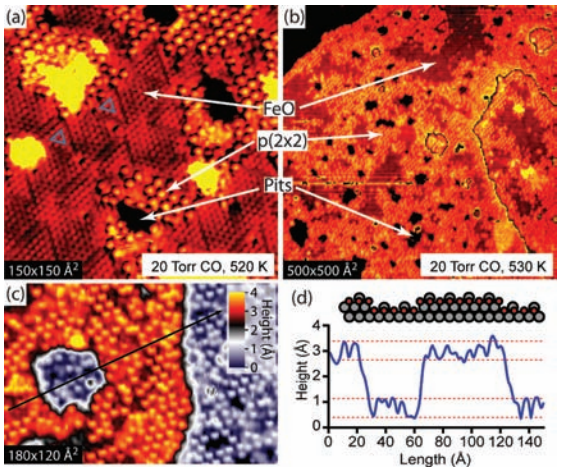

Figure 1. (a, b) Small- and large-scale STM images [(a) 0.023 V, 1.7 nA; (b) 0.22 V, 2.2 nA] of the FeO/Pt surface after 10 min exposures to 20 Torr CO at 520−530 K. These exposures resulted in the formation of a p(2 × 2) structure appearing as a hexagonal lattice of bright protrusions. Growth of this phase came at the expense of the FeO film (visible in between), which also exhibited triangular oxygen vacancy dislocation loops [marked with blue triangles in (a)], indicating partial reduction of the FeO. The p(2 × 2) phase grew near step edges and newly formed pits in the terraces. (c) STM image (0.078 V, 1.0 nA) of a CO-induced pit found near a Pt step edge. A two-level false-color scale has been used to distinguish the lower and upper layers. (d) Line profile extracted from (c), showing the apparent height and corrugation of the pit and surrounding surface. The model (side view, not to scale) shows schematically the proposed structure, where Pt (gray) is removed from the top layer and incorporated into the FeO_x film (depicted simply as red discs).

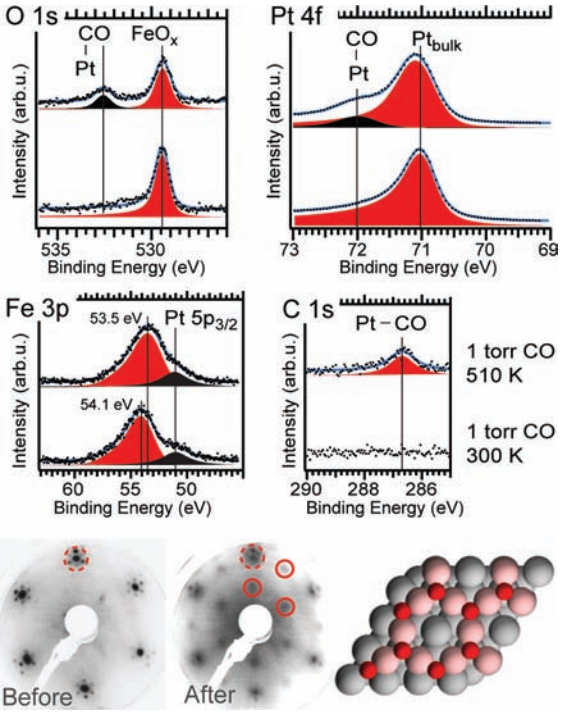

Figure 2. Ambient-pressure XPS measurements of the FeO_x film during exposure to 1 Torr CO at room temperature (lower spectra) and 510 K (upper spectra). Primary features include a reduction in FeO_x O 1s signal intensity and a shift of the Fe 3p peak to lower binding energy, indicating partial reduction of the FeO film, and the appearance of features due to adsorption of CO at Pt sites in the O 1s, Pt 4f, and C 1s spectra. Solid blue lines are least-squares fits composed of the individual peaks shown. The bottom panel displays LEED patterns measured before and after the AP-XPS measurements, showing the formation of the p(2 × 2) phase (solid red circles) at the expense of the FeO(111) phase (dashed circles). Also shown is a ball model (gray, Pt; pink, Fe; red, O) of the proposed structure, as determined by DFT+U calculations.

correction of Dudarev,[35] a five-layer Pt slab, and a p(2 × 2) surface unit cell. The experimental and computational methods are described in further detail in the Supporting Information.

STM experiments showed that exposure of the FeO/Pt(111) film to CO gas under UHV conditions (pressures up to $\sim 2 \times 10^{-5}$ Torr and temperatures up to 600 K) had no effect on the surface structure. In contrast, CO exposures at pressures of several Torr induced significant changes to the surface structure. STM images of the FeO/Pt(111) surface following exposure to CO at high pressures are depicted in Figure 1a,b. In this case, we observed patches of the hexagonal single-layer FeO structure, which initially covered the entire surface, coexisting with a new phase that appeared in the STM images as a hexagonal lattice of bright protrusions (0.8−1.2 Å apparent height). The distance between these protrusions was 5.5 Å, corresponding to a p(2 × 2) overlayer unit cell with respect to the Pt(111) substrate. The patches of FeO exhibited triangular features previously identified as oxygen vacancy dislocation loops[36] in studies where FeO films were reduced by atomic hydrogen. In these studies, the dislocation loops preceded and accompanied formation of new reduced iron oxide phases, identified as Fe_4O_3 and Fe_3O_2. The latter of these was found to consist of a p(2 × 2) honeycomb structure and to be stable against further reduction by atomic hydrogen.[24]

The p(2 × 2) phase formed upon exposure to CO was observed to nucleate near Pt step edges as well as on the terraces, where newly formed "pits" were also observed. Figure 1c displays an STM image of one of these pits, exhibiting resolved features within it. The corresponding line profile is shown in Figure 1d. It can be seen in this image and the line profile that the apparent STM height and corrugation within the pit were very similar to those of the lower terrace shown on the right side of the image, suggesting that the pits consist of areas where a single layer of Pt has been removed beneath the surface. We thus conclude that these pit structures result from extraction of Pt atoms from the underlying surface upon exposure to high-pressure CO.

In-situ XPS spectra acquired during exposure to CO at high pressure revealed more details about the restructuring of the surface. In these experiments, the pristine FeO/Pt(111) sample was placed in the AP-XPS chamber, and 1 Torr CO gas was added at room temperature. With the CO pressure fixed, the sample was then heated to the desired temperature, and XPS spectra were acquired.

The AP-XPS measurements are depicted in Figure 2, which shows O 1s, Pt $4f_{7/2}$, Fe 3p, and C 1s spectra at room temperature and at 510 K, where the reduction of the FeO film had taken place. All four room-temperature spectra acquired in CO were indistinguishable from those of pristine FeO under UHV. We therefore conclude that the FeO film is stable in 1 Torr CO at low temperature. Heating the sample to 510 K in the presence of CO led to a reduction in the intensity of the O 1s FeO_x peak at 529.4 eV by ~30% and a shift of the Fe 3p peak to 53.6 eV, which is significantly higher than the value measured for metallic Fe on Pt(111) (52.2 eV)[24] and slightly higher than that measured for the Fe_3O_2 phase formed by reduction with atomic hydrogen

dx.doi.org/10.1021/ja2015923 |J. Am. Chem. Soc. 2011, 133, 10692–10695

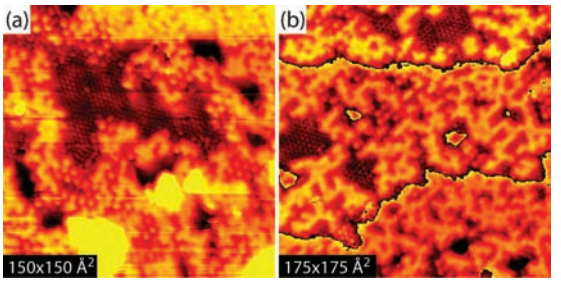

Figure 3. Decomposition of the p(2 × 2) film upon annealing in vacuum. (a) STM image (0.11 V, 1.5 nA) of the sample surface prepared by exposure to CO following annealing in vacuum at 500 K for 10 min. (b) STM image (0.093 V, 2.5 nA) of a similarly prepared surface following a brief annealing in vacuum at 600 K.

(53.1 eV).[24] The XPS results thus suggest the transformation of the FeO thin film to a partially reduced oxide phase rather than a complete reduction to Fe metal.

In addition, the O 1s spectrum at 510 K showed a second feature at 532.6 eV that appeared simultaneously with the decrease in FeO_x intensity and the shift of the Fe 3p peak. A shoulder at 71.9 eV in the Pt 4f spectrum and a new feature at 286.7 eV in the C 1s spectrum also appeared. These three new features are characteristic of CO adsorbed at Pt sites, and the binding energies suggest an atop adsorption mode.[37] The absence of additional features at ∼531 eV and ∼286 eV in the O 1s and C 1s regions, respectively, which would correspond to adsorption of CO at Pt bridge sites, indicated that the newly exposed Pt did not take the form of open (111) facets but rather was dispersed in such a way that only a single type of site was accessible.[37,38] Low-energy electron diffraction (LEED) patterns obtained before and after the CO treatment are also presented in Figure 2 (bottom left), and they show the development of a p(2 × 2) phase at the expense of the FeO(111) phase, providing a good correlation with the STM results. Thus, on the basis of the combination of STM, XPS, and LEED results, we propose that CO adsorbs at Pt adatoms in the pockets of a Fe_3O_2 honeycomb phase. A ball model of the p(2 × 2) adatom structure, following structural optimization with DFT+U calculations, is depicted in Figure 2 (bottom right).

Our experiments furthermore indicate that the presence of adsorbed CO is not only necessary for the formation the observed Fe_3O_2−Pt structure but also important in stabilizing it. STM images obtained after the CO-induced structure was heated in vacuum for 10 min at 500 K and for a few seconds at 600 K are depicted in Figure 3a,b, respectively. These STM images reveal that the structure decomposed in the absence of CO, with the Pt atoms beginning to grow into continuous islands formed between patches of FeO_x. The measured heights of these islands were consistent with monolayer Pt adjacent to FeO (as can be deduced from the typical apparent heights of 1.2−1.5 Å for the submonolayer FeO islands), further supporting the structural assignment presented above.

The reason for the formation of the Pt adatoms within Fe_3O_2 pocket sites was clarified by DFT+U calculations, as summarized in Figure 4. Here, for simplicity, we computed the total energies of several configurations with identical atomic compositions based on the Fe_3O_2 structure previously found to be stable upon reduction.[24] It was found that in the absence of CO, extraction of a Pt atom from the surface and inclusion into the honeycomb pocket site is highly unfavorable energetically, by 0.97 eV when a

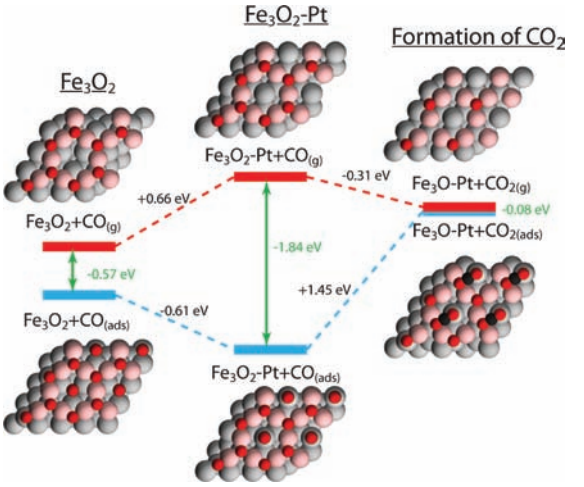

Figure 4. Schematic showing the relative energetics of different atomic configurations based on the Fe_3O_2 structure in the presence (blue) and absence (red) of adsorbed CO/CO_2, as determined by DFT+U calculations. Adsorption energies of CO and CO_2 are indicated in green.

Pt vacancy is left in the first Pt layer and 0.66 eV when the vacancy moves to the second layer. However, the situation changes completely in the presence of CO. On the Fe_3O_2 structure without Pt adatoms, CO adsorbs preferentially in the pockets of the honeycomb, with an adsorption energy of −0.57 eV. When a Pt atom is pulled out of the surface and into the pocket, however, the CO adsorption energy increases to −1.71 eV with a Pt vacancy in the first layer and −1.84 eV with the vacancy located in the second layer. This large increase in CO adsorption energy is sufficient to overcome the energetic cost of vacancy creation, making the Pt abstraction exothermic by −0.61 eV. Aggregation of the vacancies thus formed into monolayer pits, as observed in the STM images, would be expected to stabilize the Pt adatom structure even further than estimated here.

The calculations also indicated that the Pt adatom structure with adsorbed CO should be stable against removal of oxygen: reaction of the adsorbed CO molecule with an O atom from Fe_3O_2 to form gas-phase CO_2 was calculated to be endothermic by 1.53 eV and hindered by a large activation barrier of 1.77 eV, making the process highly unfavorable and improbable at the moderate temperatures employed here. This explains why the complete reduction was not observed with STM and XPS.

The inclusion of Pt adatoms in the honeycomb pockets of the Fe_3O_2 structure and their stabilization by adsorbed CO, as observed here, is similar to the CO-induced roughening of pure Pt single-crystal surfaces, which is also at least partly linked to the increase in CO binding energy at undercoordinated atoms.[4] Mutual repulsion between adsorbed CO molecules, which additionally contributes to the roughening of Pt surfaces,[39,40] is also likely to be relevant, as this would prevent aggregation of the Pt atoms and decomposition of the Fe_3O_2 honeycomb structure, which was observed upon annealing under UHV conditions.

We have thus demonstrated for the first time that exposure of a metal-supported oxide monolayer to high-pressure CO may lead to significant restructuring at the interface, resulting in a structure with metal atoms mixed into the monolayer. The formation of such a structure on a catalyst surface, which may be likely under reducing conditions and in the presence of CO (such as those employed in the preferential oxidation of CO in hydrogen for

purification of H_2), may have a profound effect on the reactivity of the catalyst. In the present case, the Pt adatom structure appears to stabilize the undercoordinated Fe atoms in the Fe_3O_2 structure (each of these being coordinated to two O atoms), potentially preserving these sites for reversible adsorption of reactants. The fact that these sites are located directly adjacent to Pt atoms, where CO is adsorbed, further suggests the possibility for a dual-site Langmuir−Hinshelwood CO oxidation mechanism, where CO adsorbed at the Pt site reacts with an oxidizing species adsorbed at the Fe site, thus eliminating competition between the reactants for adsorption sites. Indeed, it has recently been shown by Fu et al.[21] that undercoordinated Fe atoms at the edges of FeO nanoclusters on Pt(111) provide adsorption sites for O_2 on CO-saturated surfaces, enabling CO oxidation at low temperatures. Finally, the structure revealed here offers an alternative explanation for the high PROX activity observed for the high-surface-area Fe−Pt catalyst by Fu et al.[21] in their article about FeO nanoclusters. Further studies in this direction may provide valuable insight into the operation of this and similar bimetallic catalysts.

■ ASSOCIATED CONTENT

Supporting Information. Experimental and computational details and methods, XPS spectra with quantification and fit parameters, and complete ref 28. This material is available free of charge via the Internet at http://pubs.acs.org.

■ AUTHOR INFORMATION

Corresponding Author
fbe@inano.au.dk

Present Addresses
[#]Division of Synchrotron Radiation Research, Department of Physics, Lund University, Box 118, S-221 00 Lund, Sweden.
[▽]Department of Chemical Engineering, Stanford University, Stanford, CA 94305.

■ ACKNOWLEDGMENT

We gratefully acknowledge financial support of the iNANO Center by the Danish Research Agency, the Strategic Research Council, the Danish Council for Independent Research, the Carlsberg Foundation, the Villum Kahn Rasmussen Foundation, Haldor Topsøe A/S, and the European Research Council through an Advanced ERC Grant to F.B. Work at the University of Wisconsin-Madison was supported by DOE-BES, Chemical Sciences Division. Supercomputing time was utilized at NERSC, PNNL, ORNL, and ANL, all supported by the DOE. The Advanced Light Source is supported by the Director, Office of Science, Office of Basic Energy Sciences, U.S. Department of Energy, under Contract DE-AC02-05CH11231.

■ REFERENCES

(1) Ertl, G. *Surf. Sci.* **1994**, *299/300*, 742.
(2) Van Hove, M. A.; Somorjai, G. A. *Surf. Sci.* **1994**, *299/300*, 487.
(3) Over, H.; Kim, Y. D.; Seitsonen, A. P.; Wendt, S.; Lundgren, E.; Schmid, M.; Varga, P.; Morgante, A.; Ertl, G. *Science* **2000**, *287*, 1474.
(4) Thostrup, P.; Christoffersen, E.; Lorensen, H. T.; Jacobsen, K. W.; Besenbacher, F.; Nørskov, J. K. *Phys. Rev. Lett.* **2001**, *87*, No. 126102.
(5) Vestergaard, E. K.; Vang, R. T.; Knudsen, J.; Pedersen, T. M.; An, T.; Lægsgaard, E.; Stensgaard, I.; Hammer, B.; Besenbacher, F. *Phys. Rev. Lett.* **2005**, *95*, No. 126101.
(6) Tao, F.; Salmeron, M. *Science* **2011**, *331*, 171.
(7) Greeley, J.; Mavrikakis, M. *Nat. Mater.* **2004**, *3*, 810.
(8) Liu, X.; Korotkikh, O.; Farrauto, R. *Appl. Catal., A* **2002**, *226*, 293.
(9) Watanabe, M.; Zhu, Y.; Uchida, H. *J. Phys. Chem. B.* **2000**, *104*, 1762.
(10) Hirschl, R.; Delbecq, F.; Sautet, P.; Hafner, J. *Phys. Rev. B.* **2002**, *66*, No. 155438.
(11) Ma, T.; Fu, Q.; Su, H.-Y.; Liu, H.-Y.; Cui, Y.; Wang, Z.; Mu, R.-T.; Li, W.-X.; Bao, X.-H. *ChemPhysChem* **2009**, *10*, 1013.
(12) Toda, T.; Igarashi, H.; Uchida, H.; Watanabe, M. *J. Electrochem. Soc.* **1999**, *146*, 3750.
(13) Xu, Y.; Ruban, A. V.; Mavrikakis, M. *J. Am. Chem. Soc.* **2004**, *126*, 4717.
(14) Wang, C.; Daimon, H.; Sun, S. *Nano Lett.* **2009**, *9*, 1493.
(15) Healey, T.; Devries, P. D. U.S. Pat. Appl. 2007/0183968 A1, 2007.
(16) Basinska, A.; Maniecki, T. P.; Jóźwiak, W. K. *React. Kinet. Catal. Lett.* **2006**, *89*, 319.
(17) Kotobuki, M.; Watanabe, A.; Uchida, H.; Yamashita, H.; Watanabe, M. *J. Catal.* **2005**, *236*, 262.
(18) Sun, Y. N.; Qin, Z. H.; Lewandowski, M.; Carrasco, E.; Sterrer, M.; Shaikhutdinov, S.; Freund, H. J. *J. Catal.* **2009**, *266*, 359.
(19) Sun, Y.-N.; Giordano, L.; Goniakowski, J.; Lewandowski, M.; Qin, Z.-H.; Noguera, C.; Shaikhutdinov, S.; Pacchioni, G.; Freund, H.-J. *Angew. Chem., Int. Ed.* **2010**, *49*, 4418.
(20) Giordano, L.; Lewandowski, M.; Groot, I. M. N.; Sun, Y.-N.; Goniakowski, J.; Noguera, C.; Shaikhutdinov, S.; Pacchioni, G.; Freund, H.-J. *J. Phys. Chem. C.* **2010**, *114*, 21504.
(21) Fu, Q.; Li, W.-X.; Yao, Y.; Liu, H.; Su, H.-Y.; Ma, D.; Gu, X.-K.; Chen, L.; Wang, Z.; Zhang, H.; Wang, B.; Bao, X. *Science* **2010**, *328*, 1141.
(22) Nilekar, A. U.; Alayoglu, S.; Eichhorn, B.; Mavrikakis, M. *J. Am. Chem. Soc.* **2010**, *132*, 7418.
(23) Huang, W. X.; Ranke, W. *Surf. Sci.* **2006**, *600*, 793.
(24) Knudsen, J.; Merte, L. R.; Grabow, L. C.; Eichhorn, F. M.; Porsgaard, S.; Zeuthen, H.; Vang, R. T.; Lægsgaard, E.; Mavrikakis, M.; Besenbacher, F. *Surf. Sci.* **2010**, *604*, 11.
(25) Lægsgaard, E.; Besenbacher, F.; Mortensen, K.; Stensgaard, I. *J. Microsc. (Oxford, U.K.)* **1988**, *152*, 663.
(26) Salmeron, M.; Schlögl, R. *Surf. Sci. Rep.* **2008**, *63*, 169.
(27) Ogletree, D. F.; Bluhm, H.; Hebenstreit, E. D.; Salmeron, M. *Nucl. Instrum. Methods Phys. Res., Sect. A* **2009**, *601*, 151.
(28) Bluhm, H.; et al. *J. Electron Spectrosc. Relat. Phenom.* **2006**, *150*, 86.
(29) Weiss, W.; Somorjai, G. A. *J. Vac. Sci. Technol., A* **1993**, *11*, 2138.
(30) Vurens, G. H.; Salmeron, M.; Somorjai, G. A. *Surf. Sci.* **1988**, *201*, 129.
(31) Galloway, H. C.; Benitez, J. J.; Salmeron, M. *Surf. Sci.* **1993**, *298*, 127.
(32) Kresse, G.; Furthmüller, J. *Comput. Mater. Sci.* **1996**, *6*, 15.
(33) Kresse, G.; Furthmüller, J. *Phys. Rev. B.* **1996**, *54*, 11169.
(34) Perdew, J. P.; Wang, Y. *Phys. Rev. B.* **1992**, *45*, 13244.
(35) Dudarev, S. L.; Botton, G. A.; Savrasov, S. Y.; Humphreys, C. J.; Sutton, A. P. *Phys. Rev. B.* **1998**, *57*, 1505.
(36) Merte, L. R.; Knudsen, J.; Grabow, L. C.; Vang, R. T.; Lægsgaard, E.; Mavrikakis, M.; Besenbacher, F. *Surf. Sci.* **2009**, *603*, L15.
(37) Björneholm, O.; Nilsson, A.; Tillborg, H.; Bennich, P.; Sandell, A.; Hernnäs, B.; Puglia, C.; Mårtensson, N. *Surf. Sci.* **1994**, *315*, L983.
(38) Montano, M.; Bratlie, K.; Salmeron, M.; Somorjai, G. A. *J. Am. Chem. Soc.* **2006**, *128*, 13229.
(39) Tao, F.; Dag, S.; Wang, L.-W.; Liu, Z.; Butcher, D. R.; Salmeron, M.; Somorjai, G. A. *Nano Lett.* **2009**, *9*, 2167.
(40) Tao, F.; Dag, S.; Wang, L.-W.; Liu, Z.; Butcher, D. R.; Bluhm, H.; Salmeron, M.; Somorjai, G. A. *Science* **2010**, *327*, 850.